Available online at www.sciencedirect.com
ScienceDirect
Trans. Nonferrous Met. Soc. China 29(2019) 588−594
Transactions of Nonferrous Metals Society of China
www.tnmsc.cn

Yielding and fracture behaviors of coarse-grain/ultrafine-grain heterogeneous-structured copper with transitional interface

Yan-fei WANG[1], Ming-sai WANG[1], Kun YIN[1], Ai-hui HUANG[1], Yu-sheng LI[2], Chong-xiang HUANG[1]

1. School of Aeronautics and Astronautics, Sichuan University, Chengdu 610065, China;
2. Nano and Heterogeneous Structural Materials Center, School of Materials Science and Engineering, Nanjing University of Science and Technology, Nanjing 210094, China

Received 1 February 2018; accepted 19 June 2018

Abstract: Heterogeneous-structured Cu samples composed of coarse-grained (CG) and ultrafine-grained (UFG) domains with a transitional interface were fabricated by friction stir processing, in order to investigate the effect of interface constraint on the yielding and fracture behaviors. Tensile test revealed that the synergetic strengthening induced by elastic/plastic interaction between incompatible domains increases with increasing the area of constraint interface. The strain distribution near interface and the fracture morphology were characterized using digital image correlation technique and scanning electron microscopy, respectively. Fracture dimples preferentially formed at the interface, possibly due to extremely high triaxial stress and strain accumulation near the interface. Surprisingly, the CG domain was fractured by pure shear instead of the expected voids growth caused by tensile stress.

Key words: heterogeneous structure; interface; constraint; synergetic strengthening; fracture

1 Introduction

Inspired by the novel multi-scale structures of natural biomaterials, growing attention is being paid to designing new metallic materials with heterogeneous structures, such as gradient, laminated and multimodal materials [1−12]. Some combinations of superior strength, ductility and other mechanical properties have been reported. WU et al [3−5] revealed extraordinary strain hardening and synergetic strengthening from the interaction and mutual constraint between grain-size gradient surface layers and the coarse-grained (CG) core in IF-steel. Plastic strain partitioning between nanostructured (NS) and CG layers effectively inhibited the fast strain localization and cracking of brittle components, which ensured a high tensile ductility for laminated structure [6−9]. In addition, the activation of more hard slip systems by triaxial stress status and enhanced accumulation of geometrically necessary dislocations (GNDs) near interfaces were capable of significantly improving the mechanical properties [3,6,13]. However, the deformation mechanism and coupling between mechanically incompatible domains and their effect on mechanical behaviors of these heterogeneous materials are still not well understood, especially during the yielding and failure processes.

It is believed that the interfaces between incompatible domains play the critical roles in shaping the allocation and distribution of both stress and strain in heterogeneous materials [6−8]. The elastic/plastic and plastic stable/unstable interfaces in gradient material migrate dynamically during tensile testing, which makes it difficult to focus on the effect of interface [3]. MA et al [7,14] fabricated CG/NS laminates using accumulative roll bonding (ARB) and characterized their deformation and fracture process near the interfaces. However, artificial defects in the extrinsic interface were unavoidable in the ARB-processed samples and extreme sharp mechanical incompatibility across interface caused mechanical singularities during deformation, such as cracks and microvoids. Therefore, it is preferable to use cleaner interface with transitional microstructure to investigate the mechanical effects of interface constraint on the yielding and fracture behaviors of heterogeneous materials.

Foundation item: Projects (11672195, 51301092) supported by the National Natural Science Foundation of China; Project (2016JQ0047) supported by Sichuan Youth Science and Technology Foundation, China
Corresponding author: Chong-xiang HUANG; Tel: +86-28-85412106; E-mail: chxhuang@scu.edu.cn
DOI: 10.1016/S1003-6326(19)64967-8

In the present study, a novel heterogeneous structure composed of CG and ultrafine-grained (UFG) domains with an intrinsic interface is fabricated using friction stir processing (FSP). Tensile samples with varying UFG volume fraction and interface area are specially designed and tested, in order to reveal the influence of interface on synergetic strengthening. The fracture mechanisms dominated by interface constraint are discussed in terms of the observed fracture morphologies and the measured strain distribution near interface.

2 Experimental

Commercially pure Cu plate with thickness of 3 mm was annealed at 600 °C for 2 h to achieve CG base metal (BM), and then subjected to FSP under cold flowing water to produce recrystallized string zone (SZ) and the curved interface between SZ and BM, i.e. the heterogeneous structure [15]. The FSP tool has a shoulder in diameter of 8 mm and a threaded cylindrical pin in diameter of 3.0 mm and length of 1.3 mm. The structural heterogeneity of as-processed sample was carefully characterized using transmission electron microscopy (TEM) and scanning electron microscopy (SEM) equipped with electron backscatter diffraction (EBSD). Figure 1 shows the cross-section morphology of as-processed heterogeneous material. As verified later, the clear contrast between BM and bowl-shaped SZ domains suggests great difference between their microstructures, and the SZ is characterized with homogeneous UFG [16].

Two groups of dog-bone shaped tensile specimens with various UFG volume fractions and interface areas were machined from as-processed samples. To maximize the mechanical effect of interface constraint, the positions and cross-sectional dimensions of the first group were selected with the principle that ensures precise UFG volume fraction and at the same time as much constraint interface as possible. Another group of samples maintain a constant interface area that is much smaller than that of the first group. For simplicity, the first group of samples with volume fraction (x) of UFG and more constraint interface area were labeled as S_x^{M}, and the second group samples with limited interface area were correspondingly labeled as S_x^{L}. The colored frames in Fig. 1 illustrate the detailed position and cross-sectional dimension of some tensile samples. The S_x^{L} samples (dotted frames) were designed with identical thickness and interface area, but different UFG fractions. However, both the width and thickness of the S_x^{M} samples (solid frames) are varied, in order to ensure as large interface area as possible. All tensile tests were repeated at least 3 times at a nominal strain rate of 5×10^{-4} s^{-1} and room temperature.

To evaluate the interface effect on fracture response, the strain distribution across the interface in the necking stage was recorded by digital image correlation (DIC) method. In addition, the fracture geometry and morphology across the interface were elaborately examined by SEM.

3 Results and discussion

3.1 Heterogeneous structure

As the cross-sectional morphology shown in Fig. 1, no crack, porosity or other processing flaws are detected in the as-processed heterogeneous sample. Figure 2(a) shows a gradual transition of the microstructure from the SZ domain on the left side to the BM domain on the right side. The width of this transition zone is ~190 μm. The SZ domain has a typical UFG structure with an average grain size of ~710 nm, as shown in Fig. 2(b). Besides, no obvious microtexture formed in the SZ. Figure 2(c) shows the TEM image of SZ, confirming the equiaxed UFG with clear and sharp grain boundaries [17]. The hardness of SZ was rather homogeneous and measured as HV ~111.3, which was much higher than that of the BM (HV ~74.5). Similar results were revealed by XUE et al [15] and XU et al [18] that the hard SZ with recrystallized UFG microstructure was produced by reducing the heat inputting condition such as low rotational speed of stirring pin and additional water cooling during FSP.

Here the convex contour of the interface between SZ and BM (Fig. 1) can be considered as a stationary intrinsic interface between mechanically incompatible CG and UFG domains. Accordingly, the FSP-processed sample can be used as a unique heterogeneous material with an ideal transitional interface to investigate the interface effect on mechanical behaviors. The large

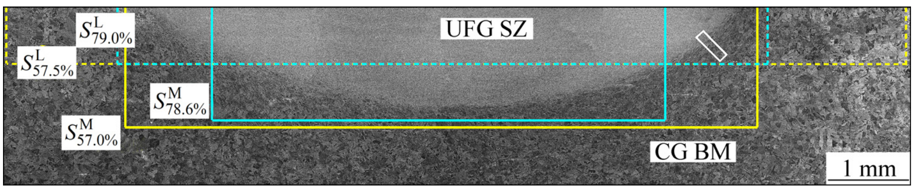

Fig. 1 Cross-sectional morphology of as-processed heterogeneous material (The solid and dotted frames illustrate the cross-section of some S_x^{M} and S_x^{L} tensile samples, respectively)

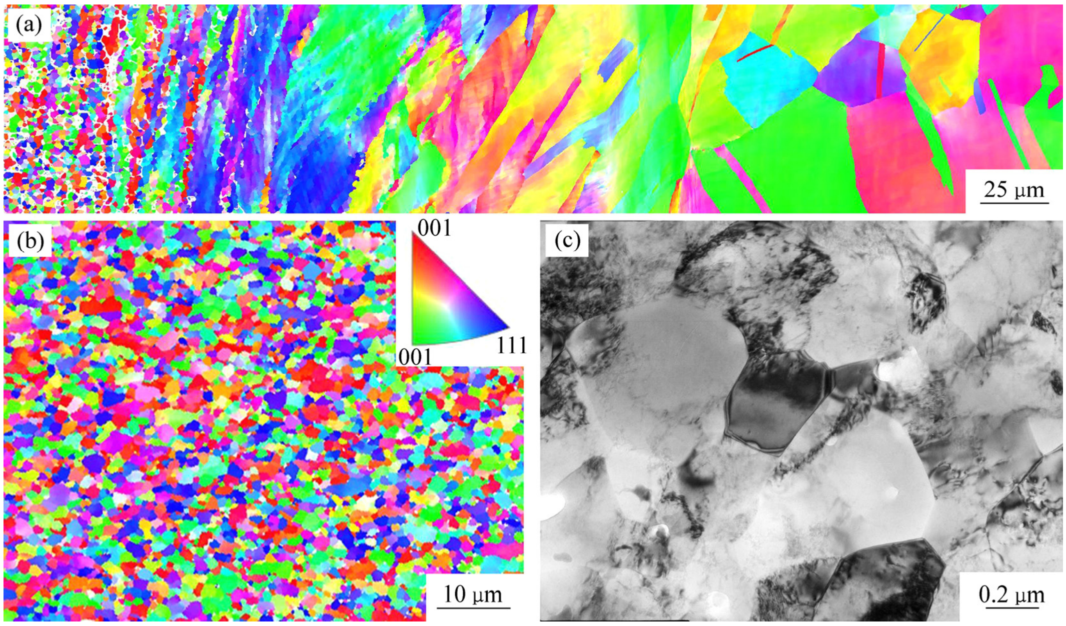

Fig. 2 Structural characteristics of FSP-processed heterogeneous material: (a) EBSD image showing UFG−CG transition (white frame in Fig. 1) between SZ (left side) and BM (right side); (b, c) EBSD image and TEM image showing UFG microstructure in SZ zone, respectively

microstructure and hardness mismatches across the interface are expected to produce stronger interaction during straining [7,19].

3.2 Strong synergetic strengthening

Figure 3(a) shows the engineering stress−strain curves of pure CG, pure UFG, heterogeneous S_x^{M} (solid lines) and S_x^{L} (dotted lines) samples. It is seen that the yield strength (0.2% ε_{p} offset stress) of heterogeneous samples increases with increasing the UFG volume fraction. The strength of S_x^{M} sample is superior to that of S_x^{L} sample with similar UFG volume fraction, while there is no obvious difference in the uniform ductility between them. The UFG component in all heterogeneous samples experienced larger uniform strain than that of homogeneous UFG bulk, especially in the $S_{20.0\%}^{\mathrm{M}}$ sample. This may indicate that such heterogeneous structural design with transitional interface is very effective in enhancing the uniform plasticity of its UFG component [6,20].

Figure 3(b) demonstrates the synergetic strengthening in heterogeneous samples. The black points are the yield strength predicted from volume-fraction-based simple rule-of-mixture (ROM) [4]. It is clear that the experimentally measured yield strengths of both S_x^{M} and S_x^{L} samples are higher than those predicted by the rule-of-mixture. In addition, the extra yield strength for the S_x^{M} samples (red line) with UFG volume fraction of 20%−70% is as high as 50 MPa, which is much higher than that for the S_x^{L} sample (blue line) with similar UFG volume fraction (<25 MPa).

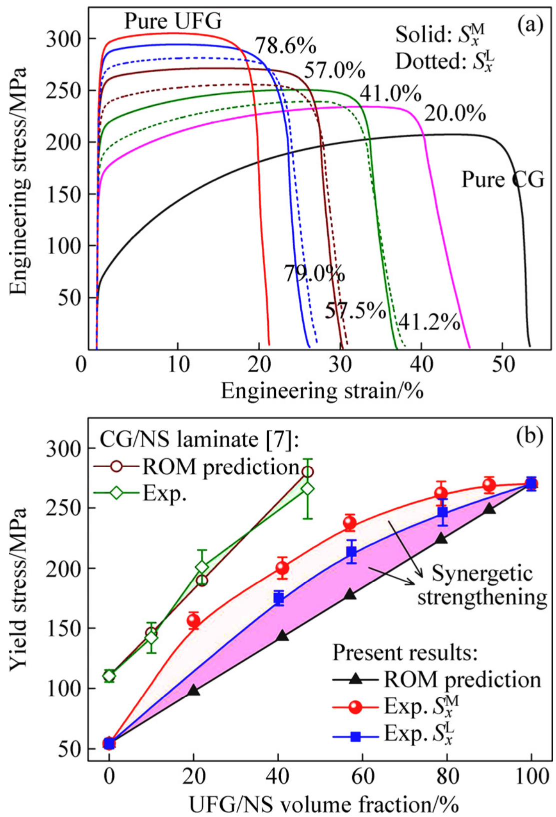

Fig. 3 Tensile stress−strain curves of heterogeneous samples with different UFG volume fractions and area of constraint interface (a) and comparison of synergetic strengthening between heterogeneous S_x^{M} and S_x^{L} samples (b) (The open data are yield strengths of CG/nanostructure (CG/NS) laminates in Ref. [7], showing almost no synergetic strengthening)

These observations not only indicate a significantly synergetic strengthening in elastic−plastic transition stage (yielding process) of the heterogeneous sample, but also suggest that the area of constraint interface is a very influential factor in strengthening and toughing heterogeneous materials [19].

Due to the incompatible lateral shrinking tendency between plastic CG (Poisson ratio $\nu\approx0.5$) and elastic UFG ($\nu\approx0.34$) domains, i.e. the effect of Poisson ratio, a strong synergetic interaction between them is expected during the yielding process of the heterogeneous sample [4,14], and thereby several strengthening mechanisms might be activated. First, the plastic shrinking of CG domain is constrained laterally by the elastically deforming UFG domain in this stage, producing triaxial tensile stress in the CG domain. In other words, the applied uniaxial stress is converted to triaxial stress state near interface, which contributes directly to increasing internal stress [21]. Second, the strain continuity between incompatible CG and UFG domains can be realized in the form of large strain gradient at the interface, which needs the accumulation of GNDs [6,10]. The orderly accumulation of GNDs will produce back stress, which can effectively strengthen materials by offsetting the applied shear stress in a long range, i.e. back-stress strengthening [5,22]. Therefore, a significant synergetic strengthening effect can be achieved in the heterogeneous samples.

It is also reasonable that the extra yield strength observed in the S_x^{M} samples is higher than that of the S_x^{L}, because a higher interface density (large area of interface) in the S_x^{M} samples permits more room for accumulating GNDs and more intense constraint between domains [1,19]. Note that, as the open data shown in Fig. 3(b), there was no extra strength in CG/nanostructure laminates which have artificial sharp interfaces [7]. This indicates that the transitional interface without any defects should have played the key role in producing high synergetic strengthening. In other words, the present transitional intrinsic interface is more effective in improving internal constraint stress and accommodating strain incompatibility between heterogeneous domains than the artificial sharp interfaces in laminates [9].

3.3 Unique fracture behavior

Figures 4(a) and (b) present the strain fields in the necking stage of the sample $S_{20.0\%}^{\mathrm{M}}$ in the tensile (ε_y) and sample width (ε_x) directions, respectively. It is seen that the UFG domain exhibits more serious strain localization than the CG domain. As marked by the black arrows in the ε_x field (Figs. 4(b)), two strain bands with ultra-high shrinking strain originated from interfaces and

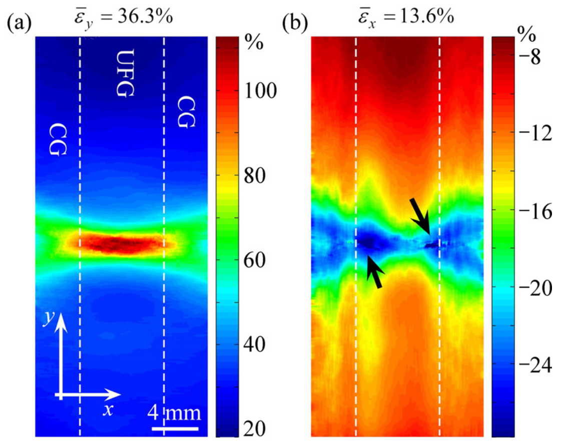

Fig. 4 Strain fields measured in necking stage of heterogeneous sample ($S_{20.0\%}^{\mathrm{M}}$): (a) Strain in tensile direction (y), ε_y; (b) Strain in width direction (x), ε_x (The dotted white lines indicate the position of interfaces, and the black arrows mark the strain bands originated from interfaces)

propagated preferentially toward UFG layer, implying the trace of crack nucleation and propagation in the early stage of fracture.

Figure 5(a) shows the typical fracture surface of a heterogeneous sample ($S_{41.0\%}^{\mathrm{M}}$). It is clear that the CG and UFG domains are separated by the curved interface. The fracture surface of the UFG domain is characterized by dense dimples (Fig. 5(b)), while the CG part exhibits a smooth surface with no dimples but individual shallow microvoids (Fig. 5(c)). Interestingly, several big and deep dimples are observed at the interface, which are not equiaxed but elliptical with the longitudinal axis parallel to the interface, as indicated by the white arrows in Fig. 5(b). Figure 5(d) presents the fracture angle, which was pictured by cutting off another half of sample. It is surprising that both the CG and UFG domains fractured in shear mode in their thickness direction with an angle of about 45° with respect to the interface plane. These observations suggest that the transitional interface and unique stress states that resulted from cross-interface interaction played a significant role in the failure process, because the above mentioned phenomena were never observed in the conventional homogeneous materials. For example, CG metals usually fracture by dimples, and UFG/NS materials fracture in shear mode but along the width direction of sample [23].

Generally, microvoids in ductile material can grow and coalesce to large dimples only when the growth parameter (A) reaches the critical value (A_{c}) [24−26]:

$$A=\varepsilon_{\mathrm{p}}\exp(\sigma_{\mathrm{m}}/\sigma_0) \tag{1}$$

where ε_{p} and σ_{m} are accumulated effective plastic strain and triaxial stress level around microvoids, respectively; σ_0 is the yield strength. It is reasonable that the plastic

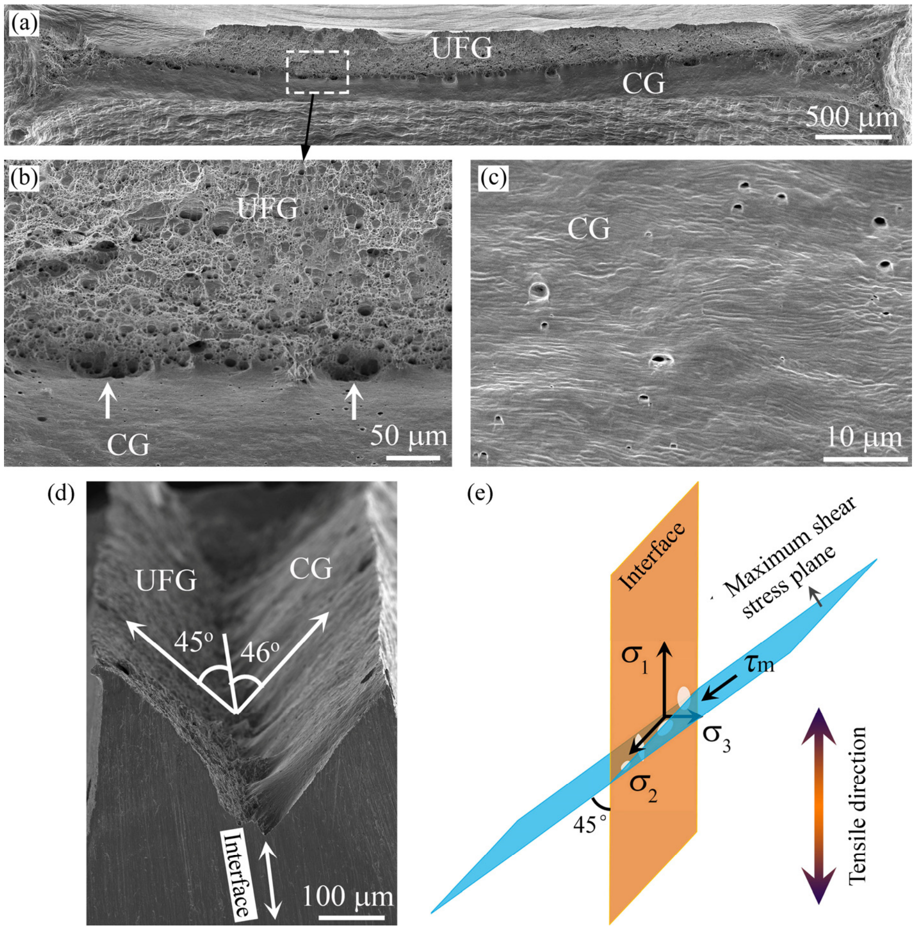

Fig. 5 Fracture behaviors of heterogeneous sample ($S^{\mathrm{M}}_{41.0\%}$): (a) Entire fracture morphology; (b) Magnified image showing large dimples at CG/UFG interface as indicated by white arrows; (c) Typical fracture surface of CG domain characterized by very smooth surface only with several microvoids; (d) Fracture angle between interface and CG/UFG domains pictured by cutting off another half of sample (The double-arrowed line in (d) marks the interface plane); (e) Illustration of stress state in front of early crack

damage, such as big dimples (Figs. 5(a) and (b)), took place preferentially at the interface, because both high level of internal stress and plastic strain (Fig. 4(b)) can be accumulated there from the interaction of CG and UFG domains during deformation [6,22]. At the same time, the high back stress can contribute to a high σ_{m} of the heterogeneous sample as well, which facilitated the nucleation of microvoids in the CG domain [24,27]. However, the effective plastic strain (ε_{p}) of CG domain, i.e. another key factor according to Eq. (1), would not be high enough for the further growth of microvoids, because the actual fracture strain in heterogeneous sample is smaller than that of pure CG sample (Fig. 3(a)). As a result, the microvoids nucleate, but cannot grow into dimples in the CG domain.

Shear fracture occurs in homogeneous material when the maximum shear stress (τ_{m}) is greater than the critical shear stress (τ_{c}) [24]

$$\tau_{\mathrm{m}} \geq \tau_{\mathrm{c}} \tag{2}$$

where τ_{c} is a constant at certain temperature. During the tensile fracture of homogeneous ductile materials, the initial crack plane is usually perpendicular to the loading direction of the tested sample, and the τ_{m} is difficult to reach τ_{c} for shear fracture before cracks propagate and coalesce to form a large crack with its size that is comparable to the cross section of sample [27]. In this study, the nucleation of early cracks in heterogeneous sample is at the interface, and the propagation direction is along the interface, as evidenced by the big elliptical dimples in Fig. 5(b). Based on this observation, it could be decided that the direction for the maximum principal stress (σ_1) in the front of cracks is parallel to the applied loading axis and the minimum principal stress (σ_3) should be perpendicular to the interface plane, and the lateral constraint stress acts as the intermediate principle stress (σ_2), as illustrated in Fig. 5(e). Thus, it is obtained

$$\tau_{\mathrm{m}} = \frac{\sigma_1 - \sigma_3}{2} \tag{3}$$

and the maximum shear stress plane is inclined by 45° to the interface [24,28]. In the current heterogeneous sample, the τ_m near interface must increase rapidly to the level of the τ_c, while the stress in other stress plane (e.g., the normal cross-section) of both CG and UFG domains is not high enough to dominate fracture. Therefore, shear fracture took place in both UFG and CG domains.

The above unique fracture behaviors highlight the role of interface in raising and reshaping internal stress, accumulating plastic strain and then controlling crack orientation. It should be noted that the present extraordinary dimples at interface and shear fracture along thickness direction were also not observed in laminates with sharp interfaces. For instance, the brittle/ductile laminated steel with well-bonded interfaces that was fabricated by hot rolling exhibited a 0º fracture angle between layers and no obvious dimples at interfaces [29]. This indicates that the transitional interface is more effective in accumulating plastic strain and passivating early crack expansion than sharp interface.

4 Conclusions

(1) The synergetic strengthening induced by elastic/plastic interaction between the CG and UFG domains contributed to higher tensile yield strength than that which is predicted by rule-of-mixture. Importantly, the synergetic strengthening increases with increasing interface area.

(2) The unique stress state, high triaxial stress and preferential accumulation of strain near transitional interface resulted in big dimples at interface and pure shear fracture along the sample thickness direction in both CG and UFG domains. The current work provided new sight into the interface-dominated strengthening effect and failure process in heterogeneous-structured materials.

References

[1] WU X L, ZHU Y T. Heterogeneous materials: A new class of materials with unprecedented mechanical properties [J]. Materials Research Letters, 2017, 5: 527−532.

[2] LU K. Making strong nanomaterials ductile with gradient [J]. Science, 2014, 345: 1455−1456.

[3] WU X L, JIANG P, CHEN L, YUAN F P, ZHU Y T. Extraordinary strain hardening by gradient structure [J]. Proceedings of the National Academy of Sciences, 2014, 111: 7197−7201.

[4] WU X L, JIANG P, CHEN L, ZHANG J F, YUAN F P, ZHU Y T. Synergetic strengthening by gradient structure [J]. Materials Research Letters, 2014, 2: 185−191.

[5] YANG M X, PAN Y, YUAN F P, ZHU Y T, WU X L. Back stress strengthening and strain hardening in gradient structure [J]. Materials Research Letters, 2016, 4: 145−151.

[6] HUANG C X, WANG Y F, MA X L, YIN S, HÖPPEL H W, GÖEKEN M, WU X L, GAO H J, ZHU Y T. Interface affected zone for optical strength and ductility in heterogeneous laminate [J]. Materials Today, 2018, 21: 713−719.

[7] MA X L, HUANG C X, XU W Z, ZHOU H, WU X L, ZHU Y T. Strain hardening and ductility in a coarse-grain/nanostructure laminate material [J]. Scripta Materialia, 2015, 103: 57−60.

[8] HUANG M, FAN G H, GENG G, CAO G J, DU Y, WU H, ZHANG T T, KANG H J, WANG T M, DU G H, XIE H L. Revealing extraordinary tensile plasticity in layered Ti−Al metal composite [J]. Scientific Report, 2016, 6: 38461−38470.

[9] CHEN A Y, LI D F, ZHANG J B, SONG H W, LU J. Make nanostructured metal exceptionally tough by introducing non-localized fracture behaviors [J]. Scripta Materialia, 2008, 59: 579−582.

[10] WU X L, YANG M X, YUAN F P, WU G L, WEI Y J, HUANG X X, ZHU Y T. Heterogeneous lamella structure unites ultrafine-grain strength with coarse-grain ductility [J]. Proceedings of the National Academy of Sciences, 2015, 112: 14501−14505.

[11] MA E, ZHU T. Towards strength–ductility synergy through the design of heterogeneous nanostructures in metals [J]. Materials Today, 2017, 20: 323−331.

[12] YUAN R, BEYERLEIN I J, ZHOU C Z. Homogenization of plastic deformation in heterogeneous lamella structures [J]. Materials Research Letters, 2017, 5: 251−257.

[13] ASHBY M F. The deformation of plastically non-homogeneous materials [J]. Philosophical Magazine, 1970, 21: 399−424.

[14] MA X L, HUANG C X, MOERING J, RUPPERT M, HÖPPEL H, GÖKEN H, NARAYAN J, ZHU Y T. Mechanical properties of copper/bronze laminates: Role of interfaces [J]. Acta Materialia, 2016, 116: 43−52.

[15] XUE P, XIAO B L, MA Z Y. High tensile ductility via enhanced strain hardening in ultrafine-grained Cu [J]. Materials Science and Engineering A, 2012, 532: 106−110.

[16] WANG Y F, AN J, YIN K, WANG M S, LI Y S, HUANG C X, Ultrafine-grained microstructure and improved mechanical behaviors of friction stir welded Cu and Cu−30Zn joints [J]. Acta Metallurgica Sinica (English letters), https://doi.org/10.1007/s40195-018-0719-3.

[17] PENG H R, GONG M M, CHEN Y Z, LIU F. Thermal stability of nanocrystalline materials: Thermodynamics and kinetics [J]. International Materials Reviews, 2016, 62: 303−333.

[18] XU N, UEJI R, FUJII H. Enhanced mechanical properties of 70/30 brass joint by rapid cooling friction stir welding [J]. Materials Science and Engineering A, 2014, 610: 132−138.

[19] WANG Y F, HUANG C X, WANG M S, LI Y S, ZHU Y T. Quantifying the synergetic strengthening in gradient material [J]. Scripta Materialia, 2018, 150: 22−25.

[20] OVID'KO I A, VALIEV R Z, ZHU Y T. Review on superior strength and enhanced ductility of metallic nanomaterials [J]. Progress in Materials Science, 2018, 94: 462−540.

[21] ASARO R J. Micromechanics of crystals and polycrystals [J]. Advances in Applied Mechanics, 1983, 23: 1−115.

[22] WANG Y F, YANG M X, MA X L, WANG M S, YIN K, HUANG A H, HUANG C X. Improved back stress and synergetic strain hardening in coarse-grain/nanostructure laminates [J]. Materials Science and Engineering A, 2018, 727: 113−118.

[23] ZHANG P, QU S, YANG M X, YANG G, WU S D, LI S X, ZHANG Z F. Varying tensile fracture mechanisms of Cu and Cu−Zn alloys with reduced grain size: From necking to shearing instability [J]. Materials Science and Engineering A, 2014, 594: 309−320.

[24] NEIMITZ A. Ductile fracture mechanisms in the high-strength steel Hardox-400 microscopic observations and numerical stress-strain analysis [J]. Procedia Materials Science, 2014, 3: 270−275.

[25] RICE J R. On the ductile enlargement of voids in triaxial stress fields [J]. Journal of the Mechanics and Physics of Solids, 1969, 17: 201−217.

[26] NEIMITZ A, GRABA M, GAŁKIEWICZ J. An alternative formulation of the Ritchie-Knott-Rice local fracture criterion [J]. Engineering Fracture Mechanics, 2017, 74: 1308−1322.

[27] WILSDORF H G F. Void initiation, growth, and coalescence in ductile fracture of metals [J]. Journal of Electronic Materials, 1975, 4: 791−809.

[28] MCCLINTOCK F A. Local criteria for ductile fracture [J]. The International Journal of Fracture Mechanics, 1968, 4: 101−130.

[29] INOUE J, NAMBU S, ISHIMOTO Y, KOSEKI T. Fracture elongation of brittle/ductile multilayered steel composites with a strong interface [J]. Scripta Materialia, 2008, 59: 1055−1058.

过渡型界面对粗晶/超细晶异质结构铜屈服和断裂行为的影响

王艳飞 [1]，王明赛 [1]，殷 琨 [1]，黄爱辉 [1]，李玉胜 [2]，黄崇湘 [1]

1. 四川大学 空天科学与工程学院，成都 610065；
2. 南京理工大学 材料科学与工程学院 纳米结构材料中心，南京 210094

摘 要：为了研究界面约束对异质结构材料屈服和断裂力学性能的影响，采用搅拌摩擦加工方法制备具有过渡型界面的粗晶/超细晶纯铜式样。拉伸测试结果表明：由粗晶和超细晶力学不协调单元弹−塑性交互作用所产生的协同强化效应随约束面积的增加而增加。使用数字散斑相关方法揭示异质结构材料颈缩过程中界面区域的应变集中分布。使用扫描电子显微镜系统分析断口形貌特征。结果发现，界面区域分布有大量大尺寸韧窝，这可能是因为粗晶与超细晶的交互约束作用在界面处产生高三轴内应力和塑性应变累积。此外，还发现粗晶区域通过剪切方式断裂，而不是拉伸应力所引起的韧窝生长机制。

关键词：异质结构材料；界面；约束；协同强化；断裂

(Edited by Xiang-qun LI)